Journal of Medicinal Chemistry

Article

Antifungal Agents. 11. *N*-Substituted Derivatives of 1-[(Aryl)(4-aryl-1*H*-pyrrol-3-yl)methyl]-1*H*-imidazole: Synthesis, Anti-*Candida* Activity, and QSAR Studies

Roberto Di Santo, Andrea Tafi, Roberta Costi, Maurizo Botta, Marino Artico, Federico Corelli, Michela Forte, Fabiana Caporuscio, Letizia Angiolella, and Anna Teresa Palamara

J. Med. Chem., **2005**, 48 (16), 5140-5153• DOI: 10.1021/jm048997u • Publication Date (Web): 07 July 2005

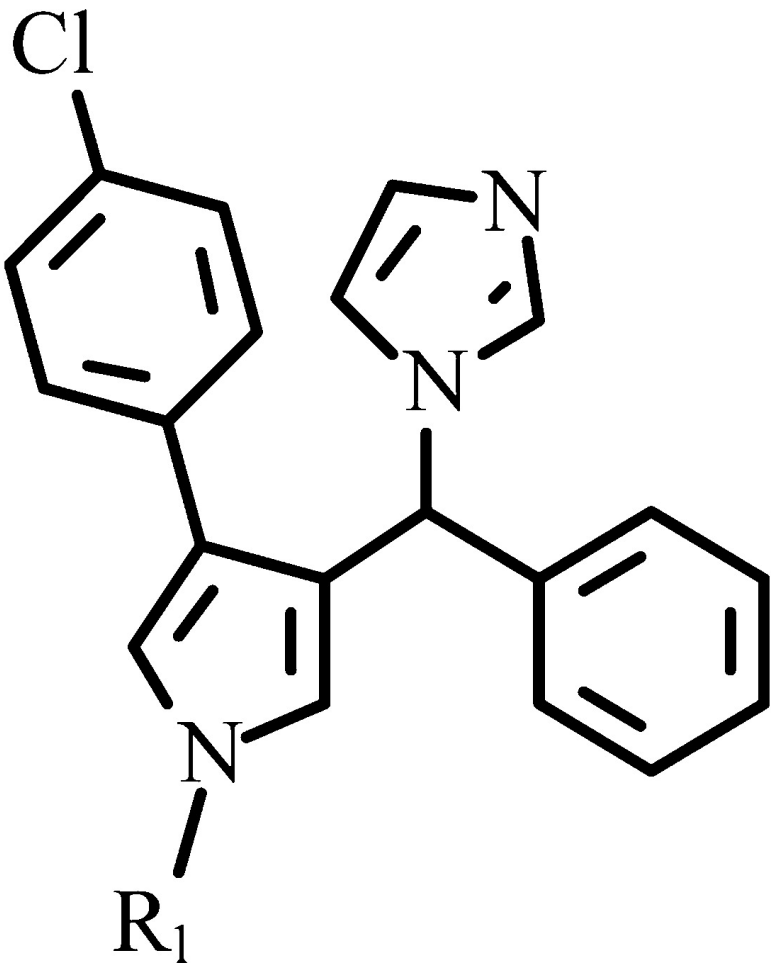

Antifungal Agents. 11. *N*-Substituted Derivatives of 1-[(Aryl)(4-aryl-1*H*-pyrrol-3-yl)methyl]-1*H*-imidazole: Synthesis, Anti-*Candida* Activity, and QSAR Studies

Roberto Di Santo,*,†,‡ Andrea Tafi,‡,§ Roberta Costi,† Maurizo Botta,*,§ Marino Artico,† Federico Corelli,§ Michela Forte,† Fabiana Caporuscio,‖ Letizia Angiolella,⊥ and Anna Teresa Palamara⊥

"Istituto Pasteur-Fondazione Cenci Bolognetti", Dipartimento di Studi Farmaceutici, Università di Roma "La Sapienza", P.le Aldo Moro 5, I-00185 Roma, Italy; Dipartimento Farmaco Chimico Tecnologico, Università di Siena, Via Aldo Moro, S. Miniato, I-53100 Siena, Italy; and Dipartimento di Studi di Chimica e Tecnologia delle Sostanze Biologicamente Attive, and Istituto di Microbiologia, Università di Roma "La Sapienza", P.le Aldo Moro 5, I-00185 Roma, Italy

Received December 10, 2004

1-[(Aryl)(4-aryl-1*H*-pyrrol-3-yl)methyl]-1*H*-imidazoles were recently reported by our group as potent anti-*Candida* agents belonging to the antifungal azole class. In the present paper the synthesis, anti-*Candida* activities, and QSAR studies on a novel series of *N*-substituted 1-[(aryl)-(4-aryl-1*H*-pyrrol-3-yl)methyl]-1*H*-imidazole derivatives are reported. The newly synthesized azoles were tested against 12 strains of *Candida albicans* together with bifonazole, miconazole, itraconazole, fluconazole, and compounds **1a**, **1b**, **3a**, **3b**, and **3c** used as reference drugs. In general, tested derivatives showed good antifungal activities, and the most potent compound was **1d** ($MIC_{90} = 0.032$ μg/mL), which was from 4- to 250-fold more potent than reference drugs. Catalyst software was applied to develop a quantitative pharmacophore model to be used for the rational design of new antifungal azoles. Some key interactions, as well as excluded volumes, further to the coordination bond of azole antifungals with the demethylase enzyme, are highlighted.

Introduction

During the past 2 decades life-threatening fungal infection frequency and type have been increasing in immunocompromised patients, such as people affected with AIDS (over 90%), bone marrow and organ transplant patients, and cancer patients.[1,2] *Candida albicans* (CA) has been identified as the major opportunistic pathogen in the etiology of fungal infections; however, the frequency of other *Candida* species is increasing.[3] The current standard of therapies are the fungicidal (but toxic) polyene, amphotericin B, and the safe (but fungistatic) azoles. In particular, the latter drugs are important antifungal agents widely used for AIDS-related mycotic pathologies.[4]

Azole antifungal agents prevent the synthesis of ergosterol, a major component of fungal membranes, by inhibiting the cytochrome P-450-dependent enzyme 14α-lanosterol demethylase (also referred as CYP51).[5,6] This enzyme contains an iron protoporphyrin unit located in its active site, which catalyzes the oxidative removal of the 14α-methyl group of lanosterol, by typical monooxygenase activity.[7] Azole antifungal agents bind to the iron of the porphyrin[8] and cause the blockade of the fungal ergosterol biosynthesis pathway, by preventing the access of the natural substrate lanosterol to the active site of the enzyme. The depletion of ergosterol and accumulation of 14α-methylated sterols alter membrane fluidity, with concomitant reduction in activity of membrane-associated enzymes and increased permeability. The net effect is to inhibit fungal growth and replication.[9]

In the last 3 decades a number of antifungal azoles were discovered and introduced in clinical practice.[10−16] Despite the important advances in this field, there is a continuing increase in the incidence of fungal infections, together with a gradual rise in azole resistance.[17] This scenario highlights the urgent need for new and effective antifungal agents. While the crystal structure of *Mycobacterium tuberculosis* CYP51 cytochrome (MT-CYP51) is known,[18] unfortunately, no three-dimensional structural information on *Candida albicans* (CA-CYP51) or other fungal CYP51 enzymes is available. Due to this fact, homology modeling[19] and pharmacophore modeling[20] techniques are currently used to attempt the rational design of new antifungal leads.

Being engaged in the last 10 years in searches on new antimycotic agents,[21−30] we reported the design and synthesis of 1-[(aryl)(4-aryl-1*H*-pyrrol-3-yl)methyl]-1*H*-imidazoles,[31] which were found to be potent anti-*Candida* agents either in vitro or in vivo assays.[32] Our SAR studies on that class of compounds, with different substituents either on the arylpyrrole moiety or on the 1-benzylimidazole portion, led us to obtain an interesting group of azole antimicrobials. Pyrrole derivatives **1a**−**7a**, **1b**, **3b**, and **3c** were in fact synthesized (Chart 1) that showed anti-*Candida* activities comparable or superior to that of miconazole, bifonazole, and ketoconazole, used as reference drugs.[33−35] It is worthy of note that **1b**, **3b**, and **3c**, the sole *N*-substituted syn-

* To whom correspondence should be addressed. R.D.S.: phone and fax, +39-6-49913150; e-mail: roberto.disanto@uniroma1.it. M.B.: phone, +39-577-234306; fax, +39-577-234333; e-mail, botta@unisi.it.
† Dipartimento di Studi Farmaceutici, Università di Roma "La Sapienza".
‡ These authors contributed equally to this work.
§ Dipartimento Farmaco Chimico Tecnologico, Università di Siena.
‖ Dipartimento SCTSBA, Università di Roma.
⊥ Istituto di Microbiologia, Università di Roma.

10.1021/jm048997u CCC: $30.25
Published on Web 07/07/2005

Chart 1. Anti-*Candida* Agents Considered as Lead Compounds **1a**−**7a**, **1b**, and **3b,c** and Newly Synthesized Derivatives **1c**−**j**, **2b,c**, **3d**−**f**, **4b**, **5b**−**e**, **6b,c**, **7b**, and **8a**−**c**

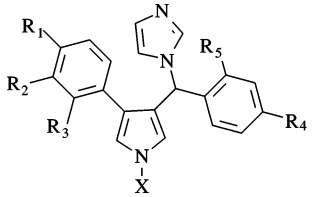

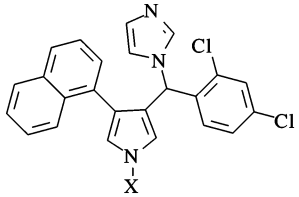

1a-j,2a-c,3a-f,4a,4b,5a-e,6a-c,7a,7b

Cmpd	R_1	R_2	R_3	R_4	R_5	X
1a	Cl	H	H	H	H	H
1b	Cl	H	H	H	H	CH_3
1c	Cl	H	H	H	H	C_2H_5
1d	Cl	H	H	H	H	C_3H_7
1e	Cl	H	H	H	H	CH_2-*c*-C_3H_5
1f	Cl	H	H	H	H	$CH{=}CH_2$
1g	Cl	H	H	H	H	CH_2-$CH{=}CH_2$
1h	Cl	H	H	H	H	CH_2-$CH{=}C(CH_3)_2$
1i	Cl	H	H	H	H	$CH{=}CH$-$COOCH_3$
1j	Cl	H	H	H	H	Ph
2a	Cl	H	Cl	H	H	H
2b	Cl	H	Cl	H	H	CH_3
2c	Cl	H	Cl	H	H	C_2H_5
3a	Cl	H	H	Cl	Cl	H
3b	Cl	H	H	Cl	Cl	CH_3
3c	Cl	H	H	Cl	Cl	C_2H_5
3d	Cl	H	H	Cl	Cl	C_3H_7

8a-c

Cmpd	R_1	R_2	R_3	R_4	R_5	X
3e	Cl	H	H	Cl	Cl	CH_2-$CH{=}CH_2$
3f	Cl	H	H	Cl	Cl	CH_2-$CH(OCH_3)_2$
4a	H	H	Cl	Cl	Cl	H
4b	H	H	Cl	Cl	Cl	CH_3
5a	Cl	H	Cl	Cl	Cl	H
5b	Cl	H	Cl	Cl	Cl	CH_3
5c	Cl	H	Cl	Cl	Cl	C_2H_5
5d	Cl	H	Cl	Cl	Cl	C_3H_7
5e	Cl	H	Cl	Cl	Cl	CH_2-$CH{=}CH_2$
6a	Cl	Cl	H	CH_3	H	H
6b	Cl	Cl	H	CH_3	H	CH_3
6c	Cl	Cl	H	CH_3	H	C_2H_5
7a	1-pyrrolyl	H	H	Cl	Cl	H
7b	1-pyrrolyl	H	H	Cl	Cl	CH_3
8a						H
8b						CH_3
8c						C_2H_5

thesized derivatives, were more active than the parent compounds **1a** and **3a**, respectively.[35] Moreover, even if we were already involved in computational studies aimed at enlightening the molecular bases of the anti-*Candida* activity of azole compounds,[34,35] at that time no systematic investigations were performed on the biological activities of the nitrogen-substituted derivatives.

In this paper, we report the synthesis and anti-*Candida* activity of a series of 1-[(aryl)(4-aryl-1*H*-pyrrol-3-yl)methyl]-1*H*-imidazoles (**1c**−**j**, **2b,c**, **3d**−**f**, **4b**, **5b**−**e**, **6b,c**, **7b**, and **8a**−**c**) bearing different substituents on the nitrogen of pyrrole ring (Chart 1, Table 1). In particular, small alkyl (methyl, ethyl, *n*-propyl, *c*-propylmethyl, dimethoxyethyl), alkenyl (vinyl, allyl, dimethylallyl, methyl 3-acryloylate) or phenyl groups were chosen. Introduction of bulky substituents was not considered on the basis of our previous experience with the *N*-2,4-dichlorobenzyl derivative of **1a** and congeners that were found to be inactive.[31] Although the newly synthesized derivatives were characterized by a stereogenic center, separation of the enantiomers was not performed. In fact, we recently demonstrated that levo and dextro forms of congeners of this series, which were separated by HPLC on polysaccharide-based chiral stationary phases, showed the same antifungal activities in in vitro tests.[25,27] In addition, taking into account that the new derivatives showed antifungal activities higher than any other compound previously synthesized by us, we applied the program Catalyst to develop a new quantitative pharmacophore model, endowed with predictive power to be used for the rational design of new antifungal azoles.

Chemistry

Phenylpyrrolylmethanones **13a**−**g**[31,32] (Table 2) were used as starting materials to obtain the new imidazole derivatives **1c**−**e,g,h,j**, **2b,c**, **3d**−**f**, **4b**, **5b**−**e**, **6b,c**, and **7b** (Scheme 1). Alkylation of pyrroles **13a**−**g** with the appropriate alkyl halide in alkaline medium (K_2CO_3) gave *N*-alkylpyrrolylmethanones **14a**−**c,e,h**−**t**. This procedure was not successful for dimethylallyl derivative **14f**, which was achieved in high yields by reaction of dimethylallyl bromide with **13a**, in the presence of NaH as a catalyst. Arylation of **13a** to afford [4-(4-chlorophenyl)-1-phenyl-1*H*-pyrrol-3-yl]phenylmethanone **14g** was performed in Suzuki reaction conditions using phenylboronic acid, Cu(II) acetate, and pyridine. The best yields were obtained in the presence of *N*-methylpyrrolidone (NMP) by microwave-assisted heating (60 W, 120 °C; 3 × 50 s). Reduction of ketones **14a**−**c,e**−**t** with $LiAlH_4$ gave methanols **15a**−**c,e**−**t**, which were then treated with 1,1′-carbonyldiimidazole (CDI) to afford the required imidazoles **1c**−**e,g,h,j**, **2b,c**, **3d**−**f**, **4b**, **5b**−**e**, **6b,c**, and **7b** (Scheme 1).

A similar synthetic pathway gave derivatives **8a**−**c** (Scheme 2). The key intermediate (2,4-dichlorophenyl)-[4-(naphthalen-1-yl)-1*H*-pyrrol-3-yl]methanone **13h** was obtained by condensation the naphthalene-1-carboxaldehyde with 2′,4′-dichloroacetophenone in aqueous sodium hydroxide to afford propenone **16**, followed by TosMIC cycloaddition in the presence of sodium hydride.

The synthesis of vinyl derivative **1f** is depicted in Scheme 3. Interestingly, the reaction of **13a** with 1,2-dichloroethane under phase transfer catalysis conditions (tetrabutylammonium hydrogen sulfate (Bu_4NHSO_4), aqueous sodium hydroxide and dichloromethane) gave the expected methanone **14d**, with a concomitant formation of dimer methanone **17**. Reduction of **14d**

Table 1. Chemical, Physical, and Analytical Data of Derivatives **1c**−**j**, **2b,c**, **3d**−**f**, **4b**, **5b**−**e**, **6b,c**, **7b**, **8a**−**c**

cmpd	R_1	R_2	R_3	R_4	R_5	X	mp (°C)	recryst solv[a]	yield (%)	reaction time (h)	chromat system[b]	analyses
1c	Cl	H	H	H	H	C_2H_5	oil	−	73	15	A	C,H,N,Cl ($C_{22}H_{20}ClN_3$)
1d	Cl	H	H	H	H	C_3H_7	oil	−	76	2	B	C,H,N,Cl ($C_{23}H_{22}ClN_3$)
1e	Cl	H	H	H	H	CH_2-*c*-C_3H_5	oil	−	79	15	B	C,H,N,Cl ($C_{24}H_{22}ClN_3$)
1f	Cl	H	H	H	H	$CH{=}CH_2$	oil	−	70	1	B	C,H,N,Cl ($C_{22}H_{18}ClN_3$)
1g	Cl	H	H	H	H	$CH_2CH{=}CH_2$	oil	−	69	1	A	C,H,N,Cl ($C_{23}H_{20}ClN_3$)
1h	Cl	H	H	H	H	$CH_2CH{=}C(CH_3)_2$	48−50	a	61	48	B	C,H,N,Cl ($C_{25}H_{24}ClN_3$)
1i	Cl	H	H	H	H	$CH{=}CHCOOCH_3$	oil	−	37	6	A	C,H,N,Cl ($C_{24}H_{20}ClN_3O_2$)
1j	Cl	H	H	H	H	Ph	oil	−	79	2	B	C,H,N,Cl ($C_{26}H_{20}ClN_3$)
2b	Cl	H	Cl	H	H	CH_3	148−150	a	60	15	A	C,H,N,Cl ($C_{21}H_{17}Cl_2N_3$)
2c	Cl	H	Cl	H	H	C_2H_5	149−151	a	59	15	A	C,H,N,Cl ($C_{22}H_{19}Cl_2N_3$)
3d	Cl	H	H	Cl	Cl	C_3H_7	123−125	b	64	15	B	C,H,N,Cl ($C_{23}H_{20}Cl_3N_3$)
3e	Cl	H	H	Cl	Cl	$CH_2CH{=}CH_2$	oil	−	62	1	A	C,H,N,Cl ($C_{23}H_{18}Cl_3N_3$)
3f	Cl	H	H	Cl	Cl	$CH_2CH(OCH_3)_2$	136−139	b	99	1	−	C,H,N,Cl ($C_{24}H_{22}Cl_3N_3O_2$)
4b	H	H	Cl	Cl	Cl	CH_3	106−108	a	28	72	A	C,H,N,Cl ($C_{21}H_{16}Cl_3N_3$)
5b	Cl	H	Cl	Cl	Cl	CH_3	oil	−	40	15	A	C,H,N,Cl ($C_{21}H_{15}Cl_4N_3$)
5c	Cl	H	Cl	Cl	Cl	C_2H_5	oil	−	63	15	A	C,H,N,Cl ($C_{22}H_{17}Cl_4N_3$)
5d	Cl	H	Cl	Cl	Cl	C_3H_7	oil	−	77	15	B	C,H,N,Cl ($C_{23}H_{19}Cl_4N_3$)
5e	Cl	H	Cl	Cl	Cl	$CH_2CH{=}CH_2$	oil	−	80	15	B	C,H,N,Cl ($C_{23}H_{17}Cl_4N_3$)
6b	Cl	Cl	H	CH_3	H	CH_3	oil	−	69	2.5	A	C,H,N,Cl ($C_{22}H_{19}Cl_2N_3$)
6c	Cl	Cl	H	CH_3	H	C_2H_5	105−106	b	71	72	A	C,H,N,Cl ($C_{23}H_{21}Cl_2N_3$)
7b	1-pyrrolyl	H	H	Cl	Cl	CH_3	oil	−	36	15	A	C,H,N,Cl ($C_{25}H_{20}Cl_2N_4$)
8a	−	−	−	−	−	H	oil	−	80	1	A	C,H,N,Cl ($C_{24}H_{17}Cl_2N_3$)
8b	−	−	−	−	−	CH_3	182−185	a	58	1	A	C,H,N,Cl ($C_{25}H_{19}Cl_2N_3$)
8c	−	−	−	−	−	C_2H_5	oil	−	63	72	A	C,H,N,Cl ($C_{26}H_{21}Cl_2N_3$)

[a] Recrystallization solvents: (a) benzene/cyclohexane, (b) cyclohexane. [b] Chromatographic system: (A) aluminum oxide/ethyl acetate, (B) aluminum oxide/chloroform.

furnished the corresponding alcohol **15d**, which was condensed with CDI to afford imidazole derivative **1f**.

At last, derivative **1i** was obtained by direct reaction of **1a** with methyl propiolate in the presence of tetrabutylammonium fluoride (Bu_4NF) (Scheme 4).

Results and Discussion

Microbiology. In Vitro Anti-*Candida* Activities. The in vitro antifungal activities of newly synthesized azole derivatives **1c**−**j**, **2b,c**, **3d**−**f**, **4b**, **5b**−**e**, **6b,c**, **7b**, and **8a**−**c** against 12 strains of *Candida albicans* are reported in Table 3 together with those of bifonazole, miconazole, itraconazole, fluconazole, and compounds **1a**, **1b**, **3a**, **3b**, and **3c** used as reference drugs.[36] Five out of 12 *Candida albicans* strains used in this study were resistant to fluconazole. With few exceptions, MIC_{50} and MIC values paralleled the related MIC_{90} data, which were chosen for a preliminary comparison between the new azoles and reference drugs. In general, the newly synthesized imidazole derivatives showed good antifungal activities when compared with reference drugs (MIC range from 0.032 to 64 μg/mL). Compounds **1d**−**i**, **2b,c**, **3e,f**, **4b**, **5c**−**e**, **6b,c**, **7b**, and **8a** were from 2 to 250 times more potent than bifonazole (MIC_{90} = 8 μg/mL), with **1d** (MIC_{90} = 0.032 μg/mL), the most active among test derivatives, being 4-, 15-, 30- and 250-fold more potent than itraconazole, fluconazole, miconazole, and bifonazole, respectively.

As a rule, the monochloro derivatives **1b**−**j** were more potent than *N*-unsubstituted compound **1a**. The best results were obtained with compounds **1b**, **1d**, and **1e** bearing methyl, propyl, or cyclopropylmethyl groups (MIC_{90} range 0.032−0.125 μg/mL). Alkenyl derivatives **1f**−**h** were just a little less potent than the above alkyl counterparts, with MIC_{90} values ranging from 0.250 to 0.5 μg/mL. Introduction of a carboxymethyl function on the vinyl group of **1f** led to acrylate **1i**, which was 16-fold less potent than the parent compound. A similar

Table 2. Chemical and Physical Data of Derivatives **13a**−**h**, **14a**−**v**, **15a**−**w**, **16**, and **17**[a]

compd	R_1	R_2	R_3	R_4	R_5	X	mp (°C)	recryst solv[b]	yield (%)	reaction time (h)	chromat system[c]
13a	Cl	H	H	H	H	−	−	−	−	−	−
13b	Cl	H	Cl	H	H	−	−	−	−	−	−
13c	Cl	H	H	Cl	Cl	−	−	−	−	−	−
13d	H	H	Cl	Cl	Cl	−	−	−	−	−	-
13e	Cl	H	Cl	Cl	Cl	−	−	−	−	−	−
13f	Cl	Cl	H	CH_3	H	−	−	−	−	−	−
13g	1-pyrrolyl	H	H	Cl	Cl	−	−	−	−	−	−
13h	−	−	−	−	−	−	210−212	a	82	0.5	−
14a	Cl	H	H	H	H	C_2H_5	oil	−	37	60	A
14b	Cl	H	H	H	H	C_3H_7	oil	−	78	7	B
14c	Cl	H	H	H	H	CH_2-*c*-C_3H_5	103−104	b	49	6	B
14d	Cl	H	H	H	H	$CH{=}CH_2$	oil	−	77	4.5	A
14e	Cl	H	H	H	H	$CH_2CH{=}CH_2$	93−94	b	32	25	A
14f	−	−	−	−	−	−	84−85	b	91	1	A
14 g	−	−	−	−	−	−	155−156	c	19	13	A
14h	Cl	H	Cl	H	H	CH_3	112−115	b	100	2	−
14i	Cl	H	Cl	H	H	C_2H_5	129−130	b	27	38	A
14j	Cl	H	H	Cl	Cl	C_3H_7	100−102	b	66	1	B
14k	Cl	H	H	Cl	Cl	$CH_2CH{=}CH_2$	oil	−	84	20	A
14l	Cl	H	H	Cl	Cl	$CH_2CH(OCH_3)_2$	81−82	b	100	24	A
14m	H	H	Cl	Cl	Cl	CH_3	oil	−	91	15	−
14n	Cl	H	Cl	Cl	Cl	CH_3	oil	−	100	4	−
14o	Cl	H	Cl	Cl	Cl	C_2H_5	123−125	b	48	26	A
14p	Cl	H	Cl	Cl	Cl	C_3H_7	80−82	b	57	2.5	B
14q	Cl	H	Cl	Cl	Cl	$CH_2CH{=}CH_2$	81−82	d	67	4	A
14r	Cl	Cl	H	CH_3	H	CH_3	oil	−	100	2	−
14s	Cl	Cl	H	CH_3	H	C_2H_5	oil	−	56	80	A
14t	1−pyrrolyl	H	H	Cl	Cl	CH_3	190−193	a	93	3	−
14u	−	−	−	−	−	CH_3	131−133	c	93	1	−
14v	−	−	−	−	−	C_2H_5	122−123	b	67	2	A
15a	Cl	H	H	H	H	C_2H_5	−	−	75	1.5	−
15b	Cl	H	H	H	H	C_3H_7	−	−	100	1	−
15c	Cl	H	H	H	H	CH_2-*c*-C_3H_5	−	−	74	5.5	−
15d	Cl	H	H	H	H	$CH{=}CH_2$	−	−	100	3.5	−
15e	Cl	H	H	H	H	$CH_2CH{=}CH_2$	−	−	100	0.5	−
15f	Cl	H	H	H	H	$CH_2CH{=}C(CH_3)_2$	−	b	92	0.5	−
15g	Cl	H	H	H	H	Ph	−	−	100	0.5	−
15h	Cl	H	Cl	H	H	CH_3	−	−	100	1	−
15i	Cl	H	Cl	H	H	C_2H_5	−	−	100	0.25	−
15j	Cl	H	H	Cl	Cl	C_3H_7	−	−	100	1	−
15k	Cl	H	H	Cl	Cl	$CH_2CH{=}CH_2$	−	−	100	2	−
15l	Cl	H	H	Cl	Cl	$CH_2CH(OCH_3)_2$	−	−	98	1.5	−
15m	H	H	Cl	Cl	Cl	CH_3	−	b	98	2	−
15n	Cl	H	Cl	Cl	Cl	CH_3	−	−	100	2	−
15o	Cl	H	Cl	Cl	Cl	C_2H_5	−	−	100	2	−
15p	Cl	H	Cl	Cl	Cl	C_3H_7	−	−	100	3	−
15q	Cl	H	Cl	Cl	Cl	$CH_2CH{=}CH_2$	−	−	100	3	−
15r	Cl	Cl	H	CH_3	H	CH_3	−	b	96	1	−
15s	Cl	Cl	H	CH_3	H	C_2H_5	−	e	86	1	−
15t	1-pyrrolyl	H	H	Cl	Cl	CH_3	−	−	96	2	−
15u	−	−	−	−	−	H	−	−	100	15	−
15v	−	−	−	−	−	CH_3	−	−	98	1	−
15w	−	−	−	−	−	C_2H_5	−	−	100	1.5	−
16	−	−	−	−	−	−	114−116	f	76	0.5	−
17	−	−	−	−	−	−	−	−	6	4.5	A

[a] Data of known derivatives **13a**−**g** are reported in ref 32. [b] Recrystallization solvents: (a) DMF/H_2O, (b) cyclohexane, (c) benzene/cyclohexane, (d) *n*-hexane, (e) benzene, (f) ethanol. [c] Chromatographic system: (A) aluminum oxide/chloroform, (B) silica gel/chloroform.

decrease of activity was noted when a phenyl moiety replaced the alkenyl group.

Generally, the introduction of one, two, or three chlorine atoms on compounds **1b**−**d** or **1g** led to alkyl derivatives **2b,c**, **3d**−**f**, **4b**, and **5b**−**e**, endowed with lower potency (MIC_{90} > 1 μg/mL). Similarly, introduction of a methyl or a pyrrolyl groups on the phenyl rings or replacement of the phenyl with a naphthalene ring led to derivatives **6b,c**, **7b**, and **8a**−**c** which showed MIC_{90} > 2 μg/mL. As an assumption, this drop in the activities could be ascribed to the highly hydrophobic groups introduced in the molecules, leading to an altered hydrophobic/hydrophilic balance.

At last, it is worthy of note that derivatives **1a**−**c,i,j**, **2b,c**, **3a,b,d**−**f**, **4b**, **5b,c**, **6b,c**, **7b**, and **8a**−**c** showed a percentage resistant strains (MIC > 64 μg/ mL) comparable to that of reference drugs, while compounds **1d**−**h** and **5e** (R% = 0) were found to be potent inhibitors of the fungal growth even on fungi strains resistant to the reference drugs.

Molecular Modeling Studies. For reasons of convenience, the azoles used in the QSAR studies [**1c**−**j**, **2b,c**, **3d**−**f**, **4b**, **5b**−**e**, **6b,c**, **7b**, **8a**−**c** (newly synthesized) and **9a**−**k**, **10a**, **11a**−**k**, **12a**−**l**, (previously synthesized)] are classified in Chart 2 as belonging to five different structural classes, named **A**, **B**, **C**, **D**, and **E**.

Scheme 1[a]

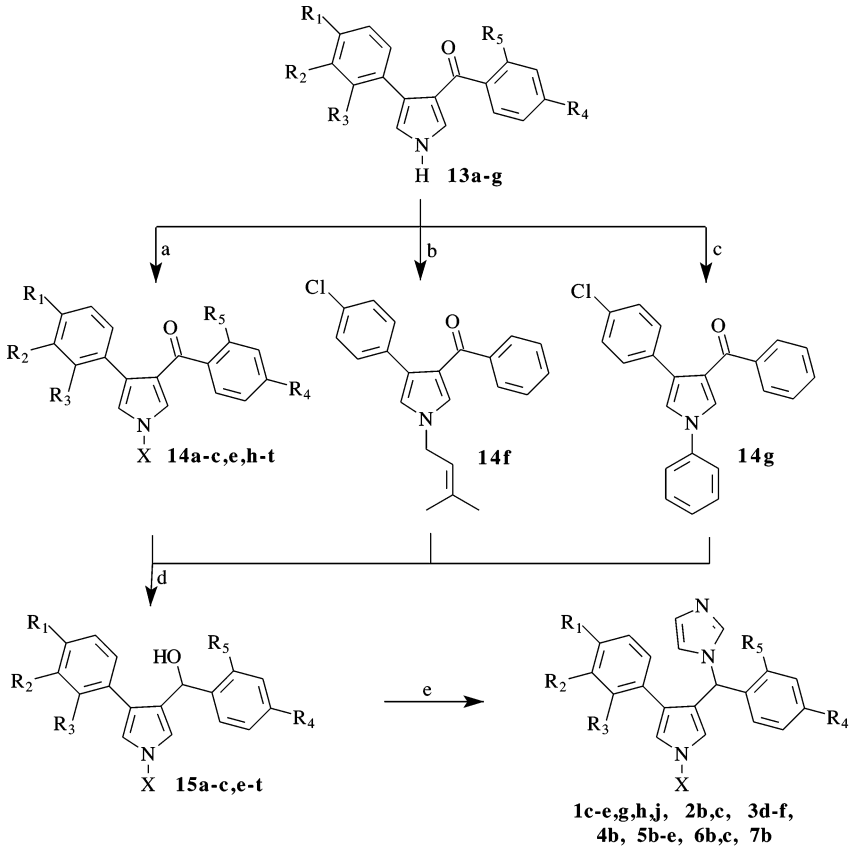

$R_1 = R_2 = R_3 = R_5 = H, Cl; R_4 = H, Cl, CH_3; X = CH_3, C_2H_5, C_3H_7, CH_2\text{-}c\text{-}C_3H_5, CH_2CH{=}CH_2, CH_2CH{=}C(CH_3)_2, CH_2CH(OCH_3)_2, Ph.$

[a] Reagents: (a) alkyl iodide or bromide, K_2CO_3, DMF; (b) 1-bromo-3-methyl-2-butene, NaH, THF; (c) $PhB(OH)_2$, $Cu(OAC)_2$, pyridine, NMP, microwave 60 W, 120 °C, 3 × 50 s; (d) $LiAlH_4$, THF; (e) 1,1′-carbonyldiimidazole, MeCN.

Scheme 2[a]

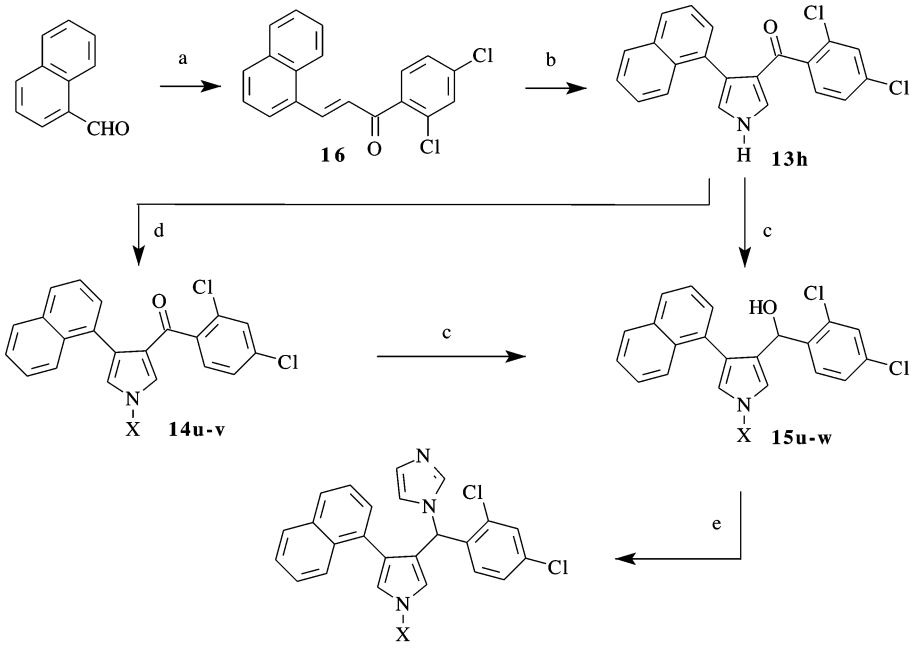

X = H, CH_3, C_2H_5

[a] Reagents: (a) 2,4-dichloroacetophenone, NaOH, EtOH; (b) toluene-4-sulfonylmethyl isocyanide (TosMIC), NaH, DMSO, Et_2O; (c) $LiAlH_4$, THF; (d) alkyl iodide, K_2CO_3, DMF; (e) 1,1′-carbonyldiimidazole, MeCN.

We have been involved since 1996 in computational studies on antifungal azoles,[34,35] and our efforts have produced remarkable results, whose soundness has been confirmed by other authors.[37] Despite these attainments, however, our work has not been able to fully satisfy our expectations for a long time. The expected

Scheme 3[a]

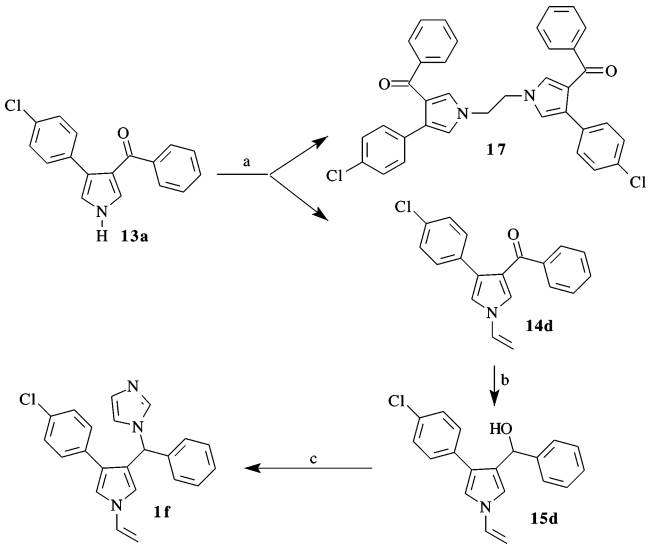

[a] Reagents: (a) 1,2-dichloroethane, Bu_4NHSO_4, NaOH, CH_2Cl_2; (b) $LiAlH_4$, THF; (c) 1,1′-carbonyldiimidazole, MeCN.

Scheme 4[a]

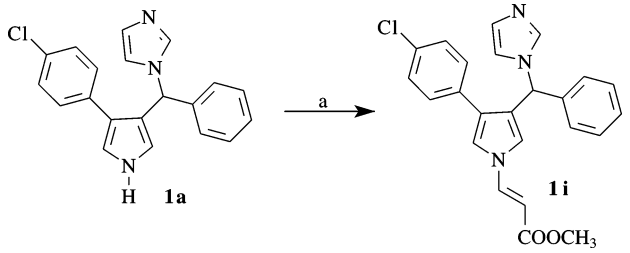

[a] Reagents: (a) methyl propiolate, Bu_4NF, THF.

predictive ability of a CoMFA model we proposed in the past,[34] in fact, was contradicted afterward by the synthesis of other analogues,[35] and a similar event recurred when—in advance of the modeling studies reported here—our subsequent pharmacophore model (HYPO1)[35] was applied to predict the activity of new derivatives **1c**−**j**, **2b,c**, **3d**−**f**, **4b**, **5b**−**e**, **6b,c**, **7b**, and **8a**−**c** (r^2_{pred} = 0.19). As a matter of fact, HYPO1's predictive fault was not surprising if one relates its framework[38] to chemical structure and antifungal activity of **1c**−**j**, **2b,c**, **3d**−**f**, **4b**, **5b**−**e**, **6b,c**, **7b**, and **8a**−**c** (Chart 1 and Table 3). MIC values of these molecules, in fact, were revealed to be strongly dependent on the presence of a substituent (possibly aliphatic) on the nitrogen of the pyrrole ring, while HYPO1 could not recognize this obviousness, as it could not match such a substituent by any of its features.

Such being the case, further pharmacophore modeling research was performed on newly and formerly synthesized azoles (see Chart 2), using the software Catalyst,[39] with the purpose to bring up to date our previous model.[38] On the occasion of this new study, the most tricky points of our former computational protocol were carefully revised, attempting to finally hit the "predictive power" target, essential for the future rational design of possibly active compounds.

First of all, the definition of the coordination feature (HYPO1's AWLP)[38] was updated and renamed UNA (unsubstituted nitrogen aromatic). Differently than AWLP, UNA was defined as a sphere; X-ray data have

Table 3. In Vitro Antifungal Activities of Imidazole Derivatives **1a**−**j**, **2b**,**c**, **3a**−**f**, **4b**, **5b**−**e**, **6b,c**, **7b**, and **8a**−**c** against *Candida albicans*

compd	%R[a]	MIC ± SD (μg/mL)	MIC_{50} (μg/mL)	MIC_{90} (μg/mL)	range (μg/mL)
1a	33.33	2.5 ± 1.45	0.125	4	0.065−4
1b	41.6	0.097 ± 0.031	0.062	0.125	0.062−0.125
1c	33.33	5.59 ± 10.97	1	8	0.25−32
1d	0	0.096 ± 0.188	0.016	0.032	0.016−0.5
1e	0	0.111 ± 0.184	0.016	0.125	0.016−0.5
1f	0	0.125 ± 0.114	0.032	0.25	0.016−0.5
1 g	0	0.082 ± 0.150	0.016	0.25	0.016−0.5
1h	0	0.194 ± 0.196	0.065	0.5	0.062−0.5
1i	16.6	1.62 ± 1.212	2	4	0.5−4
1j	50	7 ± 6.985	4	16	2−16
2b	41.6	0.46 ± 0.267	0.5	1	0.25−1
2c	41.66	1.46 ± 1.326	1	2	0.25−4
3a	33.33	4.2 ± 0.168	0.25	0.5	0.25−0.5
3b	50	1.31 ± 1.25	1	2	0.125−2
3c	25	1.5 ± 0.61	2	2	0.5−2
3d	66	8.56 ± 15.629	1	32	0.25−2
3e	33.33	0.73 ± 0.599	0.5	2	0.125−2
3f	50	2.66 ± 1.095	2	4	2−4
4b	36	1.71 ± 0.626	2	2	0.5−2
5b	16	14.6 ± 12.997	8	32	2−32
5c	41.66	1.21 ± 0.566	1	2	0.5−2
5d	100	>64	>64	>64	>64
5e	0	0.65 ± 0.709	0.25	1	0.062−2
6b	33.33	0.87 ± 0.731	0.5	2	0.25−2
6c	33.33	2.18 ± 2.419	2	2	0.125−2
7b	33.33	3.12 ± 1.246	4	4	1−4
8a	50	1 ± 0.547	0.5	2	0.5−2
8b	50	4.58 ± 5.78	4	16	0.5−16
8c	66	5.5 ± 3	4	8	2−8
bifonazole	10	3.5 ± 2.74	2	8	0.5−8
miconazole	33.33	0.65 ± 0.714	0.062	1	0.062−2
itraconazole	25	0.096 ± 0.063	0.062	0.125	0.062−0.25
fluconazole	45.45	0.24 ± 0.150	0.25	0.5	0.125−0.5

[a] Percentage of resistant strains (strains with MIC > 64 μg/mL); see Experimental Section (Microbiology) for details.

demonstrated, in fact, that the binding of azoles to CYP51 enzymes diverges to some extent from any fixed distance and angle.[40−42] Notably, similar arguments have been recently taken into account to develop a modified version of the docking program DOCK suitable for CYP enzymes.[43] Second, Catalyst's HypoRefine module,[44] which allows one to generate quantitative hypotheses with excluded volumes, thus accounting for steric hindrance problems, was used in the new computational protocol instead of HypoGen (Catalyst's original hypothesis generator). HypoGen algorithm, in fact, has been reported to possibly have difficulties in generating hypotheses that correlate well, if the steric properties of the data set make a large contribution to the activities.[44] Compounds being inactive due to incompatible steric clashes with the target might likely have their activities overpredicted by HypoGen, if they would contain the same pharmacophore as active molecules. HypoRefine, conversely, by the strategic placement of excluded volume spheres in the hypothesis, can approximate steric repulsive interactions. Finally, minimum inhibitory concentration mean values (MIC), instead of the previously used MIC_{90} values,[34,35] were preferred in this study to express the anti-*Candida* activities of the studied compounds. Although this choice restricted the comprehensive set of compounds used in the 3D-QSAR, as only formerly synthesized compounds whose MIC was known could be included, it was in agreement with the majority of the recent computational papers dealing with antifungal agents.[45] The MIC values of all the compounds (63 compounds plus flu-

Chart 2. Azoles Used in the 3D-QSAR Studies

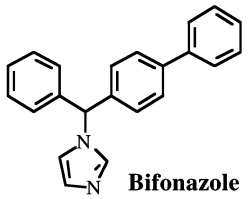

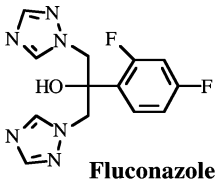

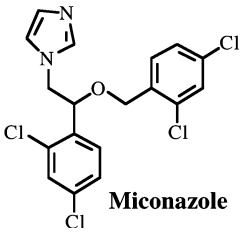

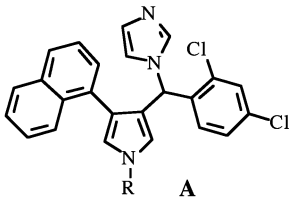

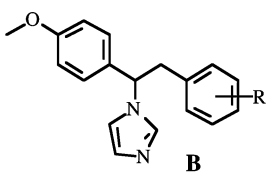

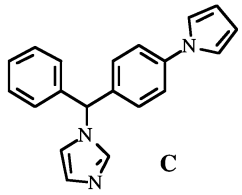

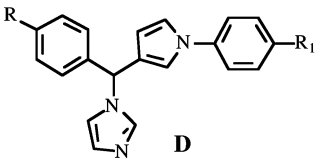

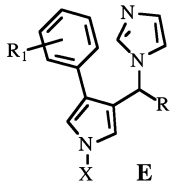

Cmpd	Scaffold	R	R_1	X
8a	A	H		
8b	A	CH_3		
8c	A	C_2H_5		
9a	B	2,4-Cl_2		
9b	B	4-NH_2		
9c	B	3-(1-pyrrolyl)		
9d	B	2-Cl		
9e	B	3-F		
9f	B	2-NO_2		
9g	B	2-(1-pyrrolyl)		
9h	B	4-NO_2		
9i	B	3-Cl		
9j	B	2-F		
9k	B	4-F		
10a	C			
11a	D	H	H	
11b	D	CH_3	H	
11c	D	Cl	Cl	
11d	D	F	Cl	
11e	D	H	Cl	
11f	D	CH_3	F	
11g	D	Cl	F	
11h	D	H	F	
11i	D	F	H	
11j	D	CH_3	Cl	
11k	D	F	F	
1a	E	Ph	4-Cl	H
1b	E	Ph	4-Cl	CH_3
1c	E	Ph	4-Cl	C_2H_5
1d	E	Ph	4-Cl	C_3H_7
1e	E	Ph	4-Cl	CH_2-*c*-C_3H_7
1f	E	Ph	4-Cl	$CH=CH_2$

Cmpd	Scaffold	R	R_1	X
1g	E	Ph	4-Cl	CH_2-$CH=CH_2$
1h	E	Ph	4-Cl	CH_2-$CH=C(CH_3)_2$
1i	E	Ph	4-Cl	$CH=CH$-$COOCH_3$
1j	E	Ph	4-Cl	Ph
2b	E	Ph	2,4-Cl_2	CH_3
2c	E	Ph	2,4-Cl_2	C_2H_5
3a	E	2,4-Cl_2-Ph	4-Cl	H
3b	E	2,4-Cl_2-Ph	4-Cl	CH_3
3c	E	2,4-Cl_2-Ph	4-Cl	C_2H_5
3d	E	2,4-Cl_2-Ph	4-Cl	C_3H_7
3e	E	2,4-Cl_2-Ph	4-Cl	CH_2-$CH=CH_2$
3f	E	2,4-Cl_2-Ph	4-Cl	CH_2-$CH(OCH_3)_2$
4b	E	2,4-Cl_2-Ph	2-Cl	CH_3
5b	E	2,4-Cl_2-Ph	2,4-Cl_2	CH_3
5c	E	2,4-Cl_2-Ph	2,4-Cl_2	C_2H_5
5e	E	2,4-Cl_2-Ph	2,4-Cl_2	CH_2-$CH=CH_2$
6b	E	4-CH_3-Ph	3,4-Cl_2	CH_3
6c	E	4-CH_3-Ph	3,4-Cl_2	C_2H_5
7b	E	2,4-Cl_2-Ph	4-(1-pyrrolyl)	CH_3
12a	E	1-naphthyl	H	H
12b	E	2-naphthyl	H	H
12c	E	2-naphthyl	H	CH_3
12d	E	1-naphthyl	H	CH_3
12e	E	2,4-Cl_2-Ph	4-Ph	H
12f	E	2,4-Cl_2-Ph	4-CF_3	H
12g	E	2,4-Cl_2-Ph	4-CN	H
12h	E	2,4-Cl_2-Ph	4-NO_2	H
12i	E	2,4-Cl_2-Ph	4-NH_2	H
12j	E	2,4-Cl_2-Ph	4-(1-pyrrolyl)	H
12k	E	2,4-Cl_2-Ph	4-OH	H
12l	E	2,4-Cl_2-Ph	4-SCH_3	H

conazole, miconazole, and bifonazole as the reference compounds), which covered 4 orders of magnitude, were normalized and formulated as $MIC_{compd}/MIC_{bifonazole}$.[34,35]

Each set of compounds considered during the hypotheses generation was cut into a training set and a complementary test set, and the MIC prediction of the latter was used as the rule to select the hypothesis representing "the pharmacophore model" among the highest scoring ones generated by Catalyst.

Because no experimental data on the biologically relevant conformations of the selected compounds were available (for example, atomic coordinates derived from X-ray crystallographic studies of their complexes with the putative receptor), we resorted to a molecular mechanics approach to build the conformational models to be used for pharmacophore generation. By means of Catalyst 2D−3D sketcher, alternative stereoisomers of all compounds were automatically generated since, in

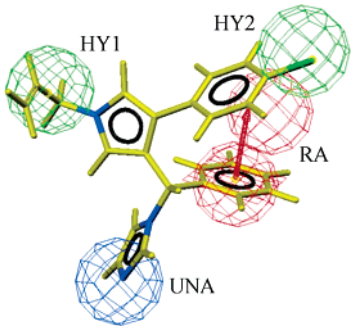

Figure 1. Compound **1g** (in yellow), the most active of the whole set, mapped onto the pharmacophore hypothesis MOD1. Pharmacophore features are color coded: blue for the unsubstituted aromatic nitrogen (UNA), red for aromatic ring (RA), green for hydrophobic (HY1 and HY2).

agreement with the synthetic pathways, the chirality of the asymmetric centers was not specified. A local minimum geometry of each compound was built and submitted to a conformational search protocol with the aim of collecting a representative set of conformers, chosen within a range of energetically reasonable conformations. The following chemical features were taken into account to build the pharmacophoric hypotheses: UNA, hydrogen-bond acceptors (HBA), hydrogen-bond donors (HBD), aromatic rings (RA), and hydrophobic groups (HY).[46] Due to both the molecules' flexibility and functional complexity, the hypothesis generator was constrained to report hypotheses with at least four features and to include UNA in each pharmacophore, to satisfy the key interaction between azole inhibitors and the enzyme.

A training set conceived to maximize the structural and microbiological information content of the whole set of studied compounds (66) was selected, accordingly to the Catalyst guidelines, to generate a three-dimensional pharmacophoric model. In particular, the following two rules were applied: (i) inclusion of the most active compound **1g** in the set, due to the fact that Catalyst pays particular attention to this molecule when it generates the chemical feature space,[47] and (ii) maximization of the kinds and relative positions (substitution pattern) of the chemical features shared by the molecules, because the program recognizes the molecules as collections of chemical features, not as assemblies of atoms or bonds. Accordingly, 24 molecules were selected out of the whole set of azole derivatives (namely, compounds **1a**, **1b**, **1d**, **1e**, **1g**, **1h**, **1i**, **1j**, **3f**, **4b**, **6b**, **8a**, **9a**, **9f**, **9j**, **10a**, **11b**, **11e**, **11h**, **12i**, **12k**, bifonazole, fluconazole, miconazole), whose activities represented all the orders of magnitude covered by each of the structural groups **A**, **B**, **C**, **D**, and **E**. The training set was characterized by MIC values spanning about 4 orders of magnitude, the minimum value 0.019 being associated with compound **1g** and the maximum value 97 associated with compound **9f**.

Further to this approach 10 hypotheses were generated by Catalyst. After a brief assessment of the statistical parameters of all 10 hypotheses, it was preferred to privilege the one with the best predictive correlation coefficient on the complementary 42 compound test set for further investigation. The selected hypothesis (named MOD1 hereafter) is displayed in Figure 1 superposed on the most active compound. It

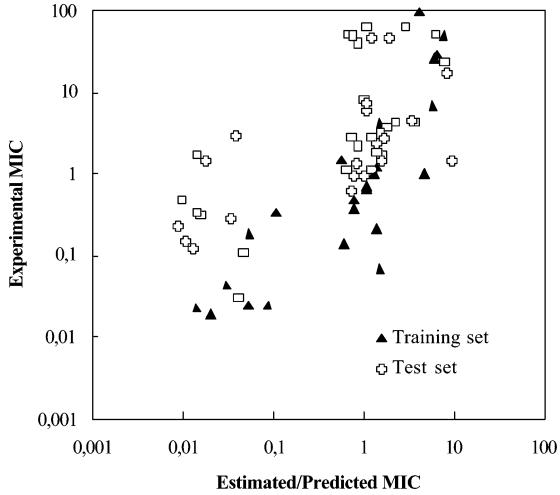

Figure 2. Regression of experimental versus estimated/predicted anti-*Candida* activities (MIC values) based on MOD1 (logarithmic scale), for each member of the training and test sets.

was the highest scoring one and consisted of four chemical features: the coordination interaction (UNA) plus one aromatic ring (RA) and two hydrophobics (HY1 and HY2). Two findings more than any other led us to credit MOD1: first of all, an interaction pattern very similar to the one proposed by this hypothesis had been already determined in a study on a series of obtusifoliol 14α-methyl demethylase azole inhibitors;[48] secondarily, and as expected, the aliphatic substituent on the pyrrole nitrogen of all the most active compounds (**1b**, **1d**, **1e**, **1f**, **1g**, **1h**) was found to match one of the two hydrophobic features (HY1).

The regression of experimental versus estimated/predicted MIC values based on MOD1 (shown in Figure 2) exhibited a correlation coefficient $r^2 = 0.84$ for the training set [root-mean-square deviation (rmsd) = 1.23]. Comparison between estimated and experimentally measured MIC values of the compounds showed, in the worst case, a 24-fold difference, while, in most cases, the comparison was inferior to a 2-fold difference. These findings indicated a reliable ability of MOD1 to estimate affinities within the training set. The execution of the same analysis on the test set revealed, differently, a less convincing scenario (see Figure 2), as a quite high correlation coefficient ($r^2 = 0.73$) did not match a homogeneous distribution of the corresponding marks around the bisector. The MIC values of several compounds were in fact predicted with very high accuracy, while the inhibitory potency of some derivatives was much overestimated (up to 2 orders of magnitude) and only one compound was underestimated (**9b**, 6.9 times). Experimental and calculated (estimated or predicted by Catalyst) MIC values of all the compounds used in the computational studies are shown in Table 4.

The prediction of the test set by MOD1 was regarded as unsatisfactory and presumed to be the after effect of possibly missing a quantitative correlation between MIC activity data of some inhibitors and their binding interaction with the enzyme active site (MIC has been found to depend on permeability and metabolic factors as well).[49] With the aim to verify the substantiality of such a guess, a reduced subset of 35 compounds out of 66 was selected for a second hypothesis generation, in

Table 4. Experimental and Estimated Anti-*Candida* Activity Values for All the Compounds Used in the 3D-QSAR Study MIC_{compd} (μmol/mL)/$MIC_{bifonazole}$ (μmol/mL)]

	$MIC_{compd}/MIC_{bifonazole}$			error	
compd	experimental	estimated (MOD1)	estimated (MOD3)	MOD1	MOD3
1a[a]	0.66	1.1	0.86	1.7	1.3
1b[a]	0.025	0.053	0.13	2.1	5.1
1c	0.11	0.018	0.016	−5.8	−6.7
1d[a]	0.023	0.014	0.0064	−1.7	−3.6
1e[a]	0.025	0.087	0.052	3.5	2.1
1f	0.031	0.041	0.26	1.3	8.3
1g[a]	0.019	0.020	0.0076	1.0	−2.5
1h[a]	0.043	0.031	0.063	−1.4	1.5
1i[a]	0.34	0.11	0.26	−3.1	−1.3
1j[a]	1.5	0.56	1.0	−2.7	−1.5
2b	0.11	0.046	0.13	−2.3	1.2
2c	0.33	0.014	0.33	−24	1.0
3a	0.92	1.0	0.58	1.1	−1.6
3b	0.28	0.034	0.60	−8.3	2.1
3c	0.31	0.016	0.063	−19	−4.9
3d	1.70	0.014	0.13	−120	−13
3e	0.15	0.011	0.045	−14	−3.3
3f[a]	0.48	0.80	0.54	1.7	1.1
4b[a]	0.36	0.80	0.28	2.2	−1.3
5b	2.9	0.039	0.28	−73	−10
5c	0.23	0.0090	0.33	−25	1.5
5e	0.12	0.013	0.23	−9.3	1.9
6b[a]	0.19	0.054	0.13	−3.6	−1.5
6c	0.47	0.0098	0.19	−48	−2.5
7b	0.62	0.74	3.3	1.2	5.4
8a[a]	0.21	1.4	0.74	6.5	3.5
8b	0.94	0.79	0.46	−1.2	−2.0
8c	1.1	0.65	0.39	−1.7	−2.8
9a[a]	1.0	1.3	0.62	1.3	−1.6
9b	1.4	9.8	26	6.9	19
9c	45	1.2	4.3	−38	−10
9d	63	2.9	23	−22	−2.8
9e	51	6.3	6.6	−8.1	−7.7
9f[a]	97	4.1	23	−24	−4.1
9g	7.8	1.0	11	−7.6	1.4
9h	17	8.4	30	−2.0	1.8
9i	44	1.9	32	−23	−1.4
9j[a]	49	7.7	22	−6.3	−2.2
9k	23	8.0	22	−2.8	−1.0
10a[a]	6.8	5.8	3.9	−1.2	−1.7
11a	2.3	1.4	21	−1.7	9.2
11b[a]	1.2	1.4	1.0	1.2	−1.2
11c	7.3	1.1	0.62	−6.4	−12
11d	2.8	1.2	0.63	−2.4	−4.4
11e[a]	0.70	1.1	0.61	1.6	−1.1
11f	3.1	1.5	0.61	−2.1	−5.1
11g	2.7	1.7	0.83	−1.6	−3.3
11i	1.8	1.4	22	−1.3	12
11h[a]	4.1	1.5	3.0	−2.7	−1.4
11j	1.1	1.2	0.68	1.1	−1.7
11k	1.4	1.6	3.7	1.2	2.7
12a	1.7	1.6	6.6	−1.1	3.8
12b	3.8	1.8	2.5	−2.2	−1.6
12c	63	1.1	15	−58	−4.0
12d	6.0	1.1	11	−5.5	1.7
12e	4.3	2.2	3.0	−1.9	−1.4
12f	2.2	0.86	0.52	−2.6	−4.3
12g	4.3	3.7	13	−1.2	3.0
12h	4.5	3.4	19	−1.3	4.2
12i[a]	28	6.5	17	−4.4	−1.7
12j	1.3	0.82	0.18	−1.6	−7.1
12k[a]	26	6.1	21	−4.2	−1.2
12l	2.8	0.74	0.92	−3.8	−3.1
bifonazole[a]	1.0	4.7	4.0	−4.7	4.0
fluconazole[a]	0.069	1.5	0.59	21	8.6
miconazole[a]	0.14	0.60	0.27	4.4	2.0

[a] Training set compounds.

which only derivatives **8a**−**c**, **9a**−**k**, **10a**, **11a**−**k**, **1b**, **1d**, **1e**, **1f**, **1g**, **1h**, bifonazole, miconazole, and fluconazole were included. The majority of the derivatives belonging to the structural class **E** (Chart 2)—covering by itself four MIC orders of magnitude—had been in fact

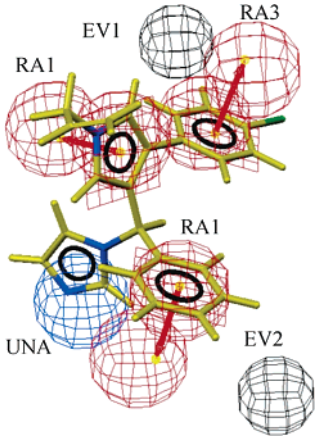

Figure 3. Compound **1g** (in yellow) mapped onto the pharmacophore hypothesis MOD2. Pharmacophore features are color coded: blue for the unsubstituted aromatic nitrogen (UNA), red for aromatic ring (RA1, RA2 and RA3). In black are shown the excluded volumes (EV1 and EV2).

steadily overestimated by MOD1, and consequently, only the six most active molecules from this class (1 order of magnitude) were considered in this generation, while the remaining 21 were arbitrarily discarded. A second set of pharmacophore hypotheses was thus built, considering a training set and a test set of, respectively, 20 and 15 compounds, from which a pharmacophore was selected (named MOD2 hereafter) according to the criteria outlined above. MOD2 showed a relevant increase of the correlation for both training set ($r^2 = 0.94$, rmsd = 0.84) and test set ($r^2 = 0.90$); however, as was to be expected owing to the rule with which the training set had been selected, the correlation coefficient decreased dramatically when all the class **E** compounds were included into an exhaustive (46 compounds) test set ($r^2 = 0.52$). MOD2 is displayed in Figure 3 superposed on **1g**. This time, the coordination interaction plus three aromatic rings (RA1, RA2, and RA3) and two excluded volumes (EV1 and EV2) were found by Catalyst to have pharmacophoric relevance. Unexpectedly, and probably due to the too close proximity that might have appeared between RA1 and a further feature on the pyrrole nitrogen substituent, HY1 was ruled out from MOD2.

The inadequate predictivity of the 46-compound exhaustive test set by MOD2 clearly demonstrated its overall unreliability. Therefore, a critical comparison was performed between this hypothesis and MOD1 to rationalize the not entirely satisfactory results obtained up to then in our studies. Two structural aspects of MOD2 appeared in fact to be really interesting and deserved some more consideration. The first unfavorable peculiarity was the presence of aromatic ring features only (RA1, RA2, and RA3) to express the attractive interactions of azoles with the amino acids of the active site of CYP51. This result was clearly a computational oversight largely induced by the exclusion from the training set of all the less active **E** compounds. As a consequence of that choice, in fact, Catalyst could recognize the relevance of different dispositions in three-dimensional space of aromatic rings (including the pyrrole, mapped by RA1) of the selected **A**, **B**, **C**, **D**, and **E** derivatives more effectively than the presence/absence of a pyrrole substituent (HY1 in MOD1), peculiar of

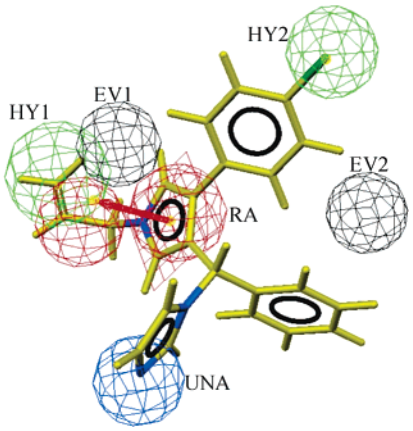

Figure 4. Compound **1g** (in yellow) mapped onto the pharmacophore hypothesis MOD3 (the final pharmacophore). Pharmacophore features are color coded: blue for the unsubstituted aromatic nitrogen (UNA), red for aromatic ring (RA), green for hydrophobic (HY1 and HY2). In black are shown the excluded volumes (EV1 and EV2).

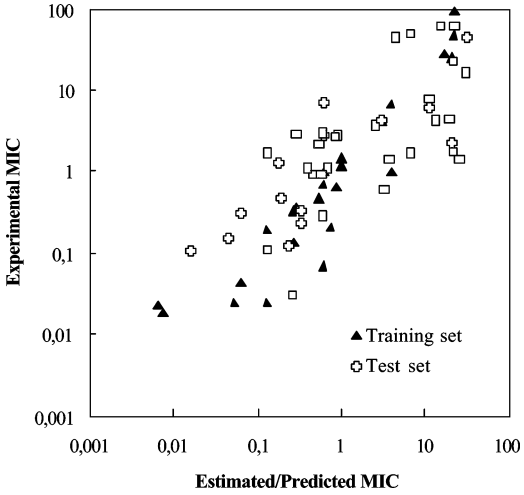

Figure 5. Regression of experimental versus estimated/predicted anti-*Candida* activities (MIC values) based on MOD3 (logarithmic scale), for each member of the training and test sets.

compounds **E**. The finding of two excluded volumes in MOD2 (EV1 and EV2) was interpreted as the second remarkable (favorably) indication provided by that hypothesis. Excluded volumes had been in fact chased since the beginning of this studies, and their appearance enforced a primal guess that the average overprediction of the 42-compound test set by MOD1 (see Figure 2) was mainly due to missing the excluded volumes in that pharmacophore. Actually, neither MOD1 nor MOD2 displayed polar features besides UNA; moreover, the possibility that steric interactions might play a relevant role in the binding of azoles into the active site of CYP51 had been already assessed both in our previous research,[35] based on the lipophilicity of our compounds and, more generally, by other authors.[19,45]

The analysis just described clarified at a molecular level the reasons for the minor reliability of MOD2 with respect to MOD1 and suggested a possible adjustment to be made to correct our computational protocol. Catalyst's default spacing value—that is, the minimum distance between actual features location—was hypothesized to be the critical control parameter that had not worked properly for our set of compounds. A further and final set of three-dimensional hypotheses was consequently generated from the first general training set, after having shortened the value of the Catalyst spacing parameter from 3.0 (default value) to 1.0 Å. The pharmacophore with the best predictivity on the test set (the highest scoring hypothesis) was then selected for further investigation and named MOD3. MOD3 (shown in Figure 4 with the most active compound **1g** superposed) was a four-features plus two excluded volumes hypothesis, which showed a remarkable increase of the correlation for the training set (24 compounds, $r^2 = 0.93$, rmsd = 0.80) with respect to MOD1. Comparison between estimated and experimental MIC values gave, in the worst case (fluconazole), a 8.5-fold difference and in most cases was inferior to a 2-fold difference. Interestingly, the regression based on MOD3 (shown in Figure 5) exhibited a correlation coefficient for the whole 42-compound test set equal to that given by MOD1 ($r^2 = 0.73$), whereas the distribution around the bisector was definitely more homogeneous than that arising from MOD1 (Figure 2), indicating the better capacity of MOD3 to predict the activities of the test set. The MIC value of all the test set compounds was in fact predicted within its measured order of magnitude, with the exception of compounds **3d**, **9b**, and **11i**, whose antifungal activity was underestimated by a factor of 13, 19, and 12, respectively.

MOD3 appears in Figure 4 as constituted by the coordination feature UNA, two hydrophobics (HY1 and HY2), one ring aromatic (RA), and two excluded volumes (EV1 and EV2). The antifungal activity of **1g** was correctly estimated by the model, due to the fact that a complete mapping of the molecule onto the pharmacophore was possible. In detail, the unsubstituted imidazole nitrogen matched UNA, the pyrrole ring RA, and the substituent on the pyrrole nitrogen HY1, while the *p*-Cl substituent was mapped by HY2. The very low MIC value of this molecule suggested that it possesses many of the molecular features required for antifungal activity. On the basis of the experimentally determined $MIC_{1g}/MIC_{bifonazole}$ (0.019, Table 4) and taking into account that the pharmacophore model correctly estimated the MIC of this compound (0.076, Table 4), one might conclude that all the pharmacophore features possibly accounted for major interactions between antifungal agents and CYP51 active site.

MOD3 accounted for the trend of the biological data associated with the compounds of both training and test sets. While the most active compounds were found to match all pharmacophoric features, the markedly decreased inhibitory activity of almost all the compounds of classes **A**, **B**, **C**, and **D** and of the less active compounds of class **E** (see Table 4) was ascribed as being due to the unmatching of pharmacophoric features. It is questionable whether the excluded volumes properly represented the surrounding atoms in the binding pocket of CA-CYP51 or more simply regions randomly selected by the HypoRefine algorithm in the aligned inactive molecules far away from the active ones that could not contain any topology.[44] Nevertheless, volume spheres helped to improve the predictivity of MOD3, as they specified spherical spaces in proximity to the pharmacophore that could not contain any atoms or

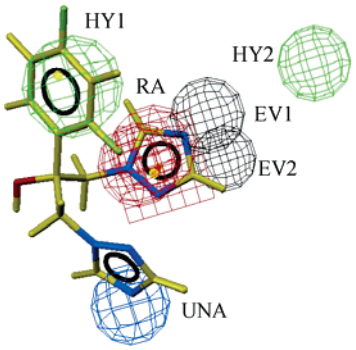

Figure 6. Fluconazole (in yellow) mapped onto the pharmacophore hypothesis MOD3 (the final pharmacophore). Pharmacophore features are color coded: blue for the unsubstituted aromatic nitrogen (UNA), red for aromatic ring (RA), green for hydrophobic (HY1 and HY2). In black are shown the excluded volumes (EV1 and EV2).

bonds, and this was a constraint preventing an advantageous matching of conformations of the less active compounds onto the pharmacophore.

The case of fluconazole could not be traced back to the general paradigm; however, it is worth of note. In Figure 6 is shown the matching of that compound onto MOD3. Due to the peculiarity of its structure, fluconazole could match only three pharmacophore features out of four: one of the two triazole rings was mapped by UNA, the second triazole by RA, and the substituted phenyl by one of the two hydrophobic features (HY1), while the fourth feature of MOD3, HY2, was too far from UNA to be possibly matched. On the other hand, Catalyst did not recognize the OH of fluconazole as a pharmacophoric feature, even though this group is actually potentially able to act both as hydrogen-bond donor and acceptor. The mismatching between MOD3 and fluconazole and the fact that the activity of fluconazole was underestimated 8.5 times by MOD3, considered together, could be an indication that the high antifungal activity of this compound might partially due to a hydrogen-bonding interaction within the active site of CA-CYP51, not recognized by our model (that consequently underestimated it). Notably, a structure-based de novo design study of inhibitors of CA-CYP51 has been recently published, based on the three-dimensional structure of a model of the enzyme built by homology modeling.[45c] In that paper is reported that a catalytically essential amino acid residue (Thr311), located on the wall of the S1 subsite of the active site (already described as one of the few hydrophilic areas in the interior of the cytochromes P450s),[50] "can act as an important candidate to form hydrogen bond with ligands". This finding indirectly strengthens our speculation.

Conclusions

The high activities showed by *N*-methyl- and *N*-ethylpyrrolyl derivatives **1b**, **3b**, and **3c** reported in previous works[31,35] led us to design and synthesize a number of derivatives of imidazoles **1**−**7a**, bearing substituents on 1-position of the pyrrole ring. The newly synthesized 1-[(aryl)(4-aryl-1-substituted-1*H*-pyrrol-3-yl)methyl]-1*H*-imidazoles (**1c**−**j**, **2b,c**, **3d**−**f**, **4b**, **5b**−**e**, **6b,c**, **7b**, and **8a**−**c**) showed high potency against *Candida albicans*, and the most active derivative was compound **1d**, which was more potent than the reference drugs. Interestingly, the cited derivatives and some congeners were found to be highly active against *Candida* strains resistant to itraconazole, bifonazole, miconazole, and fluconazole used as reference drugs.

As a summary of the 3D-QSAR studies reported in this paper, the new pharmacophore model developed and named MOD3 seems to be more definite, accurate, flexible, and realistic with respect to the model we proposed in our previous studies, as aromatic $\pi-\pi$ stacking interactions appear no more to be the sole interactions able to modulate the activities of different antifungal agents. Some key interactions, as well as excluded volumes, further to the coordination bond of azole antifungals with the demethylase enzyme are now highlighted. The pharmacophore will be validated by database searching and by the prediction of the antifungal activities of new compounds. As a matter of fact, however, a preliminary successful test of MOD3 has been allowed[51] by the recent publication of some novel anti-*Candida* agents analogues of fluoxetine.[52] This approach, hopefully, will allow us to endow our compounds with substituents able to form H-bonds within the enzyme's active site. Finally, even if the chosen approach improved considerably our previous pharmacophore, nevertheless it highlighted the inherent limitations in the use of MIC values for the development of quantitative interaction models of antifungal azoles. Soon, 3D models of CA-CYP51 will be probably available to improve this ligand-based approach and to combine it with a structure based one, to design new potent derivatives with higher probability of success. The possibility to discover a more accurate method to describe the relevant coordination interaction between the azole ring and the cytochrome heme moiety is still under study.

Finally, the hypothesis that the antifungal activity of fluconazole might partially be due to a hydrogen-bonding interaction within the active site of CA-CYP51 is quite reasonable. It strengthens and adjusts at the same time one of the conclusions of our previous pharmacophore study on azole anti-*Candida* agents.[35] In that paper we concluded that aromatic interactions with amino acids localized in proximity of heme could be responsible for the different activities of diverse antifungal agents, while hydrogen bonds or similar hydrophilic interactions (not pointed out in that study) could fortuitously increase the affinity of an inhibitor with respect to another one. The results of the studies reported here corroborate that work if we amend the above-mentioned conclusions assuming more hydrophobic than aromatic interactions, within the catalytic site of CA-CYP51.

Experimental Section

1. Chemistry. Melting points were determined on a Büchi 530 melting point apparatus and are uncorrected. Infrared (IR) spectra (Nujol mulls) were recorded on a Perkin-Elmer Spectrum-one spectrophotometer. ^{1}H NMR spectra of imidazole derivatives were recorded at 400 MHz on a Bruker AC 400 Ultrashield spectrophotometer. Column chromatographies were performed on alumina (Merck; 70−230 mesh) or silica gel (Merck; 70−230 mesh) column. All compounds were routinely checked by TLC by using aluminum-baked silica gel plates (Fluka DC−Alufolien Kieselgel 60 F_{254}). Developed plates were visualized by UV light. Solvents were reagent

grade and, when necessary, were purified and dried by standard methods. Concentration of solutions after reactions and extractions involved the use of a rotary evaporator (Büchi) operating at a reduced pressure (ca. 20 Torr). Organic solutions were dried over anhydrous sodium sulfate. Analytical results agreed to within ±0.40% of the theoretical values. The newly synthesized azole derivatives were analyzed for C, H, N, and Cl.

2. Syntheses. Specific examples presented below illustrate the general synthetic procedures. The chemical and physical properties of the newly synthesized derivatives and their intermediates are reported in Tables 1 and 2.

1-(2,4-Dichlorophenyl)-3-(naphthalen-1-yl)propenone (**16**). A mixture of naphthalene-1-carboxaldehyde (21.9 g, 140 mmol) and 2′,4′-dichloroacetophenone (26.5 g, 140 mmol) in ethanol (290 mL) was treated with a solution of sodium hydroxide (13.6 g, 340 mmol) in water (290 mL). The mixture was stirred at room temperature for 20 min and then treated with water (600 mL) and the precipitate that formed was filtered off. The filtrate was washed with water and recrystallized from ethanol to afford 34.7 g (76%) of pure **16**.

(2,4-Dichlorophenyl)[4-(naphthalen-1-yl)-1*H*-pyrrol-3-yl]methanone (**13h**). A solution of **16** (16 g, 48.9 mmol) and toluene-4-sulfonylmethylisocyanide (9.6 g, 48.9 mmol) in a mixture of anhydrous dimethyl sulfoxide/ethyl ether (150:300 mL) was added dropwise into a well-stirred suspension of sodium hydride (60% in white oil; 8.9 g, 220 mmol) in dry ethyl ether (260 mL) under argon stream. After the addition, the mixture was stirred at room temperature for 15 min and then treated with water (900 mL). The formed precipitate was filtered off, and the filtrate was washed with ethanol (3 × 50 mL) to afford pure **13h** (14.77 g, 82%).

[4-(4-Chlorophenyl)-1-propyl-1*H*-pyrrol-3-yl]phenylmethanone (**14b**). A well-stirred suspension of **13a** (1.5 g, 5.3 mmol), 1-bromopropane (4.7 g, 38 mmol), and anhydrous potassium carbonate (1.5 g, 11 mmol) in dry *N,N*-dimethylformamide (8.5 mL) was heated at 90 °C for 7 h. After cooling, the mixture was treated with water (50 mL) and extracted with ethyl acetate (3 × 100 mL). The organic extracts were collected, washed with brine (3 × 50 mL), and dried, and the solvent was evaporated under reduced pressure. The residue was chromatographed on silica gel (chloroform as eluent) to furnish pure **14b** (1.3 g, 78%).

[4-(4-Chlorophenyl)-1-(3-methyl-2-butenyl)-1*H*-pyrrol-3-yl]phenylmethanone (**14f**). A solution of **13a** (1.0 g, 3.5 mmol) in dry tetrahydrofuran (40 mL) was added dropwise into a well-stirred suspension of sodium hydride (60% in white oil; 0.14 g, 3.5 mmol) in dry tetrahydrofuran (32 mL). After the addition, the mixture was stirred at room temperature for 10 min and then a solution of 1-bromo-3-methyl-2-butene (0.5 g, 3.5 mmol) in dry tetrahydrofuran (12 mL) was added. The mixture was stirred at room temperature for 1 h and then was treated with water (100 mL). After the removal of the solvent, the residue was extracted with ethyl acetate (3 × 100 mL). The organic extracts were collected, washed with brine (3 × 50 mL), and dried, and the solvent was evaporated. The residue was chromatographed on aluminum oxide (chloroform as eluent) to furnish 1.1 g (92%) of pure **14f**.

[4-(4-Chlorophenyl)-1-ethenyl-1*H*-pyrrol-3-yl]phenylmethanone (**14d**). Into a well-stirred solution of **13a** (2.0 g, 7.1 mmol) and tetrabutylammonium hydrogen sulfate (0.24 g, 0.71 mmol) in 1,2-dichloroethane (10 mL) cooled at 0 °C was added NaOH 50% (13.5 mL). The resulting mixture was refluxed for 4.5 h, allowed to cool, diluted with water (100 mL), and extracted with ethyl acetate (3 × 150 mL). The collected organic extracts were washed with brine (3 × 100 mL) and dried, and the solvent was removed to give a yellow residue that was chromatographed on aluminum oxide (chloroform as eluent) to afford **14d** (1.68 g, 77% yield) and **17** (0.25 g, 6%).

[4-(4-Chlorophenyl)-1-phenyl-1*H*-pyrrol-3-yl]phenylmethanone (**14g**). In a 5-mL glass tube were placed **13a** (0.10 g, 0.54 mmol), cupric acetate (0.32 g, 1.8 mmol), phenylboronic acid (0.13 g, 1.1 mmol), NMP−pyridine mixture (0.5:0.5 mL), and a magnetic stir bar. The vessel was sealed with a septum and placed into the microwave cavity. Microwave irradiation of 60 W was used, the temperature being ramped from room temperature to 120 °C. Once 120 °C was reached, the reaction mixture was held at this temperature for 3 × 50 s (after each cycle, the reaction vessel was cooled and cupric acetate (1.8 mmol), phenylboronic acid (1.1 mmol), and NMP−pyridine (0.5:0.5 mL) were added). The reaction vessel was opened, the mixture was diluted with tetrahydrofuran (10 mL) and filtered off, and the solvent was evaporated. The residue was dissolved in ethyl acetate (50 mL), washed with 1 N HCl (2 × 20 mL) and then with brine (3 × 20 mL), dried, and evaporated. The crude product was chromatographed on aluminum oxide (chloroform as eluent) to furnish 0.05 g (41%) of pure **14g**.

4-(4-Chlorophenyl)-1-ethyl-α-phenyl-1*H*-pyrrole-3-methanol (**15a**). To a well-stirred suspension of lithium aluminum hydride (0.08 g, 2.0 mmol) in dry tetrahydrofuran (10 mL), at 0 °C, was added dropwise a solution of **14a** (0.43 g, 1.4 mmol) in dry tetrahydrofuran (10 mL). After the addition, the mixture was stirred at room temperature for 1.5 h and then carefully treated with crushed ice. The inorganic precipitate was removed, and the solution was concentrated and extracted with ethyl acetate (3 × 50 mL). The combined organic extracts were washed with brine (3 × 50 mL), dried, and evaporated to give **15a** (0.33 g, 75%), which was used in the following reaction without further purification.

1-[[4-(4-Chlorophenyl)-1-propyl-1*H*-pyrrol-3-yl]phenylmethyl]-1*H*-imidazole (**1d**). A solution of **15b** (1.1 g, 3.4 mmol) and 1,1′-carbonyldiimidazole (2.4 g, 15 mmol) in anhydrous acetonitrile (60 mL) was stirred at room temperature for 2 h. The solvent was removed, and the residue was dissolved in ethyl acetate (100 mL). The organic solution was washed with brine (3 × 50 mL) and dried, and the solvent was evaporated. The crude product was chromatographed on aluminum oxide (chloroform as eluent) to furnish 0.97 g (76%) of pure **1d**.

3-[3-(4-Chlorophenyl)-4-(1*H*-imidazol-1-ylphenylmethyl)-1*H*-pyrrol-1-yl]-2-propenoic Acid Methyl Ester (**1i**). A solution of 1 M tetrabutylammonium fluoride in tetrahydrofuran (5.0 mL, 5.0 mmol) was added onto a well-stirred solution of **1a** (0.83 g, 2.8 mmol) in anhydrous tetrahydrofuran (9 mL). A solution of methyl propiolate (0.35 g, 4.2 mmol) in dry tetrahydrofuran (9 mL) was added dropwise. After the addition the solution was stirred at room temperature for 6 h and then treated with water (100 mL) and extracted with ethyl acetate (3 × 150 mL). The organic solution was washed with brine (3 × 100 mL) and dried, and the solvent was evaporated. The crude product was chromatographed on aluminum oxide (ethyl acetate as eluent) to give pure **1i** (0.16 g, 37%).

3. Microbiology. Anti-*Candida* in Vitro Assays. The in vitro antifungal activities of the derivatives **1c**−**j**, **2b,c**, **3d**−**f**, **4b**, **5b**−**e**, **6b,c**, **7b**, and **8a**−**c** were tested against *Candida albicans*. The antifungal potency was evaluated by means of the minimal inhibitory concentration (MIC), using the serial test in the broth microdilution modification method published by the National Committee for Clinical Laboratory Standard (NCCLS) method M 27-A2.[36] MIC was defined as the lowest concentration of test substances at which there was no visible growth, as compared with a blank experiment, after the present incubation time. For the preparation of the dilution series, all derivatives were dissolved in dimethyl sulfoxide (DMSO) at a concentration of 6.4 mg/mL and were stored frozen at −20 °C. The solution was added to the medium at the right concentration. Further progressive double dilutions with a test medium furnished the required concentrations in the range from 0.016 to 64 μg/mL. Blanks were prepared in the test medium, without adding test substances.

Bifonazole, miconazole, itraconazole, and fluconazole were used as reference antifungal drugs. Bifonazole, miconazole, and itraconazole were dissolved in DMSO, while fluconazole was dissolved in distilled water at a concentration of 6.4 mg/mL. All microorganisms were preliminarily incubated at 28 °C for 24 h on RPMI 1640 (Sigma) medium buffered pH 7.0. Antimicrobial tests were performed with RPMI 1640 medium using inocula of approximately 10^4 cells/ mL. Readings of MICs

were taken at 24 h of growth at 28 °C. MIC values were calculated by the expression MIC = (ΣMIC_i)/s_t, where MIC_i is the minimal inhibitory concentration values of all strains at the used concentration C_i and s_t is the total number of strains. MIC_{50} and MIC_{90} refer to MIC for 50 and 90% of strains, respectively. %R refers to percentage of resistant strains at 64 μg/mL.

Twelve strains of *C. albicans,* four strains originally isolated from AIDS patients with oropharyngeal candidiasis, four isolates from HIV-infected subjects with recurrent vulvovaginitis, two reference strains (ATCC 24433 and 20891), and two laboratory strains (3153 and CA2) were employed in these studies. All the *Candida* strains used in this study has been tested for their sensitivity to bifonazole, miconazole, itraconazole, and fluconazole. Among those being fluconazole-resistant, three were derived from HIV infected patients (AIDS 68 and AIDS 126), one was an ATCC resistant strain (20891), and one was a laboratory-selected strain obtained through several passages in fluconazole-enriched medium (CO23rflu). All strains were identified by conventional diagnostic procedures.

4. Molecular Modeling. All the biological activity MIC mean values were expressed, after having converted all the μg/mL values to μmol/mL units, as $MIC_{compd}/MIC_{bifonazole}$, and they span 4 orders of magnitude.

Because no experimental data on the biologically relevant conformations of the studied compounds were available, the conformational populations to be used for the pharmacophore generation were built by the software Catalyst procedure. Training and test set compounds were submitted to both fast and best conformational searches, using the poling algorithm and the CHARMm force field as implemented in Catalyst, with the aim of collecting a representative set of conformers chosen within a range of 20 kcal/mol with respect to the global minimum. Moreover, alternative stereoisomers were automatically considered during the conformational search, since the chirality of the asymmetric center was not specified, in agreement with the synthetic pathways.

Ten hypotheses were generated for each training set after the selection of the following features: hydrophobic (HY), ring aromatic (RA), hydrogen-bond acceptor (HBA), hydrogen-bond donor (HBD), and the new defined feature "unsubstituted nitrogen aromatic" (UNA). UNA was implemented by modifying the definition of the "hydrogen-bond-acceptor lipid" feature, already present into the internal software database, so as to include only aromatic nitrogens bearing a lone pair. The N-2 atom of the triazole ring was excluded, as azole compounds do not inhibit the enzyme by coordination of that atom. The hypothesis generator was constrained to report hypotheses with at least four features and to include UNA in each pharmacophore. During the hypotheses generation, the HypoRefine algorithm was used. All the control parameters values were set to their default values except for the Spacing value, which was set to a value of 100 picometers instead of 297, and for the Variable Tolerance value, which was set to a value of 1 instead of 0, during the generation of MOD3.

A brief assessment of the statistical parameters of all 10 hypotheses was done after every generation through the cost analyses reported here. MOD1: cost = 114.8 bits. Total fixed cost (ideal hypothesis) = 95.7 bits. Cost of the null hypothesis = 140.8 bits. Cost range over the 10 best generated hypotheses = 7.1 bits. MOD2: cost = 89.4 bits. Total fixed cost (ideal hypothesis) = 82.2 bits. Cost of the null hypothesis = 131.6 bits. Cost range over the 10 best generated hypotheses = 7.6 bits. MOD3: cost = 117.3 bits. Total fixed cost (ideal hypothesis) = 109.1 bits. Cost of the null hypothesis = 140.8 bits. Cost range over the 10 best generated hypotheses = 17.5 bits.

Special care was taken to test the models for chance correlation. The three pharmacophores were evaluated for statistical significance using a randomization trial procedure derived from the Fischer method. Experimental activities of the training set were scrambled 19 times to obtain 19 spreadsheets with randomized activity data. A total of 19 hypotheses were generated using the scrambled training sets, and among the 190 resulting hypotheses (10 for each computation run), none was found with a total cost lower than the chosen hypothesis, so there was at least a 95% probability that the three hypotheses did not represent chance correlation in the data.

Test set molecules were fitted to the generated hypothesis using the Catalyst fast fit feature. Fast fit refers to the method of finding the optimum fit of the substrate to the hypothesis among all the conformers of the molecule without performing an energy minimization on the conformers of the molecule. This method was also used to fit the training set molecules to the pharmacophore.

Acknowledgment. Thanks are due to Ministero della Sanità, Istituto Superiore di Sanità, "Programma Nazionale di ricerca sull'AIDS" (grant no. 30F.19), and to Italian MIUR (PRIN 2004) for partial support. Elemental analyses were performed by Dott. M. Zancato, University of Padova, Italy.

Supporting Information Available: Spectroscopic and elemental analysis data of the newly synthesized derivatives **1c**−**j**, **2b,c**, **3d**−**f**, **4b**, **5b**−**e**, **6b,c**, **7b**, and **8a**−**c**. This material is available free of charge via the Internet at http://pubs.acs.org.

References

(1) Richardson, M. D. Opportunistic and Pathogenic Fungi. *J. Antimicrob. Chemother.* **1991**, *28* (Suppl. A), 1−11.
(2) Ablordeppey, S. Y.; Fan, P.; Ablordeppey J. H.; Mardenborough, L. Systemic Antifungal Agents Against AIDS−Related Opportunistic Infections: Current Status and Emerging Drugs in Development. *Curr. Med. Chem.* **1999**, *6*, 1151−1196.
(3) Beck-Sague, C. M.; Jarvis, W. R. Secular Trends in the Epidemiology of Nosocomial Fungal Infections in the United States, 1980−1990. *J. Inf. Dis.* **1993**, *167*, 1247−1251.
(4) Koltin, Y. Target for Antifungal Drug Discovery. *Annu. Rep. Med. Chem.* **1990**, *25*, 141−148.
(5) Ghannoum, M. A. Future of Antimycotic Therapy. *Dermatol. Ther.* **1997**, *3*, 104−111.
(6) Asai, K.; Tsuchimori, N.; Okonogi, K.; Perfect, J. R.; Gotoh, O.; Yoshida, Y. Formation of Azole-Resistant *Candida albicans* by Mutation of Sterol 14-Demethylase P450. *Antimicrob Agents Chemother.* **1999**, *43*, 1163−1169.
(7) Dawson, J. H.; Sono, M. Cytochrome P-450 and Chloroperoxidase: Thiolate-Ligated Heme Enzymes. Spectroscopic Determination of Their Site Structures and Mechanistic Implications of Thiolate ligation. *Chem. Rev.* **1987**, *87*, 1255−1276.
(8) Odds, F.; Brown, A. J. P.; Gow, N. A. R. Antifungal Agents: Mechanism of Action. *Trends Microbiol*. **2003**, *11*, 272−279.
(9) Adams, J. L.; Metcalf, B. W. Therapeutic Consequences of the Inhibition of Sterol Metabolism. In *Comprehensive Medicinal Chemistry*; Hansch, C., Sammes, P. G., Taylor, J. B., Eds.; Pergamon Press: Oxford, England, 1990; Vol. 2, pp 333−364.
(10) Buchel, K. H.; Draber, W.; Regel, E.; Plempel, M. Synthesen und Eigenschften von Clotrimazol und Weiteren Antimykotischen 1-Triphenylmethylimidazolen. (Syntheses and Properties of Clotrimazole and Further Antimycotic 1-(Triphenylmethyl)imidazoles.) *Arzneim.-Forsch.* **1972**, *22*, 1260−1272.
(11) Bannatyne, R. M.; Cheung, R. Susceptibility of *Candida albicans* to Miconazole. *Antimicrobial Agents Chemother.* **1978**, *13*, 1040−1041.
(12) Heel, R. C.; Brodgen, R. N.; Carmine, A.; Morley, P. A.; Speight, T. M.; Avery, G. S. Ketoconazole: A Review of Its Therapeutic Efficacy in Superficial and Systemic Fungal Infections. *Drugs* **1982**, *23*, 1−36.
(13) Plempel, M.; Regel, E.; Buchel, K. H. Antimycotic Efficacy of Bifonazole in Vitro and in Vivo. *Arzneim.-Forsch.* **1983**, *33*, 517−524.
(14) Richardson, K.; Brammer, K. W.; Marriott, M. S.; Troke, P. F. Activity of UK-49,858, a Bis-Triazole Derivative, Against Experimental Infections with *Candida albicans* and Trichophyton mentagrophytes. *Antimicrobial Agents Chemother.* **1985**, *27*, 832−835.
(15) George, D.; Miniter, P.; Androile, V. T. Efficacy of UK-109496, a New Azole Antifungal Agent, in an Experimental Model of Invasive Aspergillosis. *Antimicrobial Agents Chemother.* **1996**, *40*, 86−91.
(16) Espinel-Ingroff, A.; Shadomy, S.; Gebhart, R. J. In Vitro Studies with R 51,211 (Itraconazole). *Antimicrobial Agents Chemother.* **1984**, *26*, 5−9.

(17) Sanglard D.; Odds, F. C. Resistance of *Candida* Species to Antifungal Agents: Molecular Mechanisms and Clinical Consequences. *Lancet Infect. Dis.* **2002**, *2*, 73−85.
(18) Podust, L. M.; Poulos, T. L.; Waterman, M. R. Crystal Structure of Cytochrome P450 14α-Sterol Demethylase (CYP51) from *Mycobacterium tuberculosis* in Complex with Azole Inhibitors. *Proc. Natl. Acad. Sci. U.S.A.* **2001**, *98*(6), 3068−3073.
(19) Xiao, L.; Madison, V.; Chau, A. S.; Loebenberg, D.; Palermo, R. E.; McNicholas, P. M. Three-Dimensional Models of Wild-Type and Mutated Forms of Cytochrome P450 14α-Sterol Demethylase from *Aspergillus fumigatus* and *Candida albicans* Provide Insights into Posocanazole Binding. *Antimicrobial Agents Chemother.* **2004**, *48*, 568−574.
(20) De Groot, M. J.; Ekins, S. Pharmacophore Modeling of Cytochromes P450. *Adv. Drug Del. Rev.* **2002***, 54,* 367−383.
(21) Di Santo, R.; Massa, S.; Artico, M. Synthesis of Biologically Active Azoles via TosMIC. *Farmaco* **1993**, *48*, 209−229.
(22) Di Santo, R.; Massa, S.; Costi, R.; Simonetti, G.; Retico, A.; Apuzzo, G.; Troccoli, F. Antifungal Agents. VIII. Synthesis and Antifungal Activities of Bipyrryl Analogues of Bifonazole. *Farmaco* **1994**, *49*, 229−236.
(23) Di Santo, R.; Costi, R.; Artico, M.; Massa, S.; Musiu, C.; Scintu, F.; Putzolu, M.; La Colla, P. Antifungal estrogen-like imidazoles. Synthesis and antifungal activities of thienyl and 1*H*-pyrrolyl derivatives of 1-aryl-2-(1*H*-imidazol-1-yl)ethane. *Eur. J. Med. Chem.* **1997**, *32*, 143−149.
(24) Di Santo, R.; Costi, R.; Artico, M.; Massa, S.; Musiu, C.; Milia, C.; Putzolu, M.; La Colla, P. *N*-(1-Naphthylmethyl)-*N*-(1-alkyl-4-aryl-1*H*-pyrrol-3-ylmethyl)methylami nes Related To Naftifine. Synthesis And Antifungal Activity. *Med. Chem. Res.* **1997**, *7*, 98−108.
(25) Cirilli, R.; Costi, R.; Di Santo, R.; Ferretti, R.; La Torre, F.; Angiolella, L.; Micocci, M. Analytical and Semipreparative Enantiomeric Separation of Azole Antifungal Agents by High-Performance Liquid Cromatography on Polysaccharide-Based Chiral Stationary Phases. Application to In Vitro Biological Studies. *J. Chromatogr. A* **2002**, *942*, 107−114.
(26) Artico, M.; Massa, S.; Di Santo, R.; Costi, R.; Retico, A.; Apuzzo, G.; Simonetti, N. Antifungal Agents. 5. Chloro and Amino Derivatives of 1,2-Diaryl-1-(1*H*-imidazol-1-yl)ethane with Potent Antifungal Activities. *Eur. J. Med. Chem.* **1993**, *28*, 715−720.
(27) Botta, M.; Corelli, F.; Gasparrini, F.; Messina, F.; Mugnaini, C. Chiral Azole Derivatives. 4.1. Enantiomers of Bifonazole and Related Antifungal Agents: Synthesis, Configuration Assignment, and Biological Evaluation. *J. Org. Chem.* **2000**, *65*(15), 4736−4739.
(28) Massa, S.; Di Santo, R.; Retico, A.; Artico, M.; Simonetti, N.; Panico, S.; Fabrizi, G.; Lamba, D. Antifungal Agents. 1. Synthesis and Antifungal Activities of Estrogen-Like Imidazole and Triazole Derivatives. *Eur. J. Med. Chem.* **1992**, *27*, 495−502.
(29) Massa, S.; Di Santo, R.; Artico, M.; Costi, R.; Apuzzo, G. Simonetti, G.; Artico, M. Novel In Vitro Highly Active Antifungal Agents with Pyrrole and Imidazole Moieties. *Med. Chem. Res.* **1992**, *2*, 148−153.
(30) Massa, S.; Di Santo, R.; Costi, R.; Mai, A.; Artico, M.; Retico, A.; Apuzzo, G.; Artico, M.; Simonetti, G. Antifungal Agents. 4. Synthesis of *neo*-Isopyrrolnitrin and Other 3-Aryl-4-nitro-1*H*-pyrroles via TosMIC. *Med. Chem. Res.* **1993**, *3*, 192−199.
(31) Massa, S.; Di Santo, R.; Artico, M.; Costi, R.; Di Filippo, C.; Simonetti, G.; Retico, A.; Artico, M. Researches on Antibacterial and Antifungal Agents. XV. 3-Aryl-4-[α-(1*H*-imidazol-1-yl)benzyl]pyrroles with Potent Antifungal Activity. *Eur. Bull. Drug Res.* **1992**, *1*, 12−17.
(32) Artico, M.; Di Santo, R.; Costi, R.; Massa, S.; Retico, A.; Artico, M.; Apuzzo, G.; Simonetti, G.; Strippoli, V. Antifungal Agents. 9. 3-Aryl-4-[α-(1*H*-imidazol-1-yl)arylmethyl]pyrroles: A New Class of Potent Anti-*Candida* Agents. *J. Med. Chem.* **1995**, *38*, 4223−4233.
(33) Massa, S.; Di Santo, R.; Costi, R.; Simonetti, G.; Retico, A.; Apuzzo, G.; Artico, M. Antifungal Agents. III. Naphthyl and Thienyl Derivatives of 1*H*-Imidazol-1-yl-4-phenyl-1*H*-pyrrol-3-ylmethane. *Farmaco* **1993**, *48*, 725−736.
(34) Tafi, A.; Anastassopoulou, J.; Theophanides, T.; Botta, M.; Corelli, F.; Massa, S.; Artico, M.; Costi, R.; Di Santo, R.; Ragno, R. Molecular Modeling of Azole Antifungal Agents Active Against *Candida albicans*. 1. A Comparative Molecular Field Analysis Study. *J. Med. Chem.* **1996**, *39*, 1227−1235.
(35) Tafi, A.; Costi, R.; Botta, M.; Di Santo, R.; Corelli, F.; Massa, S.; Ciacci, A.; Manetti, F.; Artico, M. New Derivatives of 1-[(Aryl)-[4-aryl-1*H*-pyrrol-3-yl]methyl]-1*H*-imidazole, Synthesis, Anti-*Candida* Activity, and Quantitative Structure−Activity Relationship Studies. *J. Med. Chem.* **2002**, *45*, 2720−2732.
(36) National Committee for Clinical Laboratory Standards. 2002. Reference methods for broth dilution antifungal susceptibility testing of yeast, approved standard. NCCLS document M27-A2. National Committee for Clinical Laboratory Standards, Waine, PA.
(37) Liu, J.; Pan, D.; Tseng, Y.; Hopfinger, A. J. 4D-QSAR Analysis of a Series of Antifungal P450 Inhibitors and 3D-Pharmacophore Comparisons as a Function of Alignment. *J. Chem. Inf. Comput. Sci.* **2003**, *43*, 2170−2179.
(38) HYPO1 was composed by one ad hoc defined aromatic-nitrogen-with-lone-pair vectorial feature (AWLP) to simulate the coordination interaction of azole inhibitors with the iron atom of the enzyme protoporphyrin system and three aromatic rings.[35]
(39) *Catalyst 4.8*, Accelrys, Inc.: 9685 Scranton Road, San Diego, CA.
(40) Poulos, T. L.; Howard, A. J. Crystal Structures of Methyrapone- and Phenylimidazole-Inhibited Complexes of Cytochrome P-450cam. *Biochemistry* **1987**, *26*, 8165−8174.
(41) Yano, J. K.; Koo, L. S.; Shuller, D. J.; Li, H.; Ortiz De Montellano, P. R.; Poulos, T. L. Crystal Structure of a Thermophilic Cytochrome P450 from the Archaeon *Sulfolobus solfataricus*. *J. Biol. Chem.* **2000**, *275*, 31086−31092.
(42) Podust, L. M.; Poulos, T. L.; Waterman, M. R. Crystal Structure of Cytochrome P450 14alpha-Sterol Demethylase (Cyp51) from *Mycobacterium tubercolosis* in Complex with Azole Inhibitors. *Proc. Natl. Acad. Sci. U.S.A.* **2001**, *98*, 3086−3073.
(43) Verras, A.; Kuntz, I. D.; Ortiz De Montellano, P. R. Computer-Assisted Design of Selective Imidazole Inhibitors for Cytochrome P450 Enzymes. *J. Med. Chem.* **2004**, *47*, 3572−3579.
(44) http://www.accelrys.com/catalyst/hyporefine.html.
(45) (a) Sharma, P.; Rane, N.; Gurram, V. K. Synthesis and QSAR Studies of Pyrimido[4,5-*d*]pyrimidine-2,5-dione derivatives as Potential Antimicrobial Agents. *Bioorg. Med. Chem.* **2004**, *14*, 4185−4190. (b) Gollapudy, R.; Ajmani, S.; Kulkarni, A. Modling and Interaction of *Aspergillus fumigatus* Lanosterol 14-α Demethylase with Azole Antifungals. *Bioorg. Med. Chem.* **2004**, *12*, 2937−2950. (c) Ji H.; Zhang W.; Zhang M.; Kudo M.; Aoyama Y.; Yoshida Y.; Sheng C.; Song Y.; Yang S.; Zhou Y.; Lü J.; Zhu J.; Structure-Based de Novo Design, Synthesis, and Biological Evaluation of Non-Azole Inhibitors Specific for Lanosterol 14α-Demethylase of Fungi. *J. Med. Chem.* **2003**, *46*, 474−85. (d) Wiktorowicz, W.; Markuszewski, M.; Krysinski, J.; Kaliszan, R. Quantitative Structure−Activity Relationships Study of a Series of Imidazole derivatives as Potential New Antifungal Drugs. *Acta Pol. Pharm.* **2002**, *59*, 295−306.
(46) Greene, J.; Kahn, S. D.; Savoj, H.; Sprague, P.; Teig, S. L. Chemical Function Queries for 3D Database Search. *J. Chem. Inf. Comput. Sci.* **1994**, *34*, 1297−1308.
(47) Catalyst 4.5 Tutorials, August 1999, Molecular Simulation, Inc., San Diego, CA 92121.
(48) Bargar, T. M.; Secor, J.; Markley, L. D.; Shaw, B. A.; Erickson, J. A. A Comparative Molecular Field Analysis of Obtusifoliol 14α-Methyl Demethylase Inhibitors. *Pestic. Sci.* **1999**, *55*, 1059−1069.
(49) Upadhayaya, R. S.; Sinha, N.; Jain, S., Kishore, N., Chandra, R.; Arora, S. K. Optically Active Antifungal Azoles: Synthesis and Antifungal Activity of (2*R*,3*S*)-2-(2,4-Difluorophenyl)-3-(5-[2-[4-aryl-piperazin-1-yl]-ethyl]-tetrazol-2-yl/1-yl)-1-[1,2,4]-triazol-1-yl-butan-2-ol. *Bioorg. Med. Chem.* **2004**, *12*, 2225−38.
(50) Hasemann, C. A.; Kurumbail, R. G.; Boddupalli, S. S.; Peterson, J. A.; Deisenhofer, J. Structure and Function of Cytochromes P450: A Comparative Analysis of Three Crystal Structures. *Structure* **1995**, *2*, 41−62.
(51) Unpublished results.
(52) Silvestri, R.; Artico, M.; La Regina, G.; Di Pasquali, A.; De Martino, G.; D'Auria, F. D.; Nencioni, L.; Palamara, A. T. Imidazole Analogues of Fluoxetine, a Novel Classs of Anti-*Candida* Agents. *J. Med. Chem.* **2004**, *47*, 3924−3926.

JM048997U